

Towards Precision Spectroscopy of Baryonic Resonances

Michael Döring^{1,2,*}, Maxim Mai^{1,3,4}, and Deborah Rönchen^{3,4}

¹George Washington University, Washington, DC 20052, USA

²Thomas Jefferson Accelerator Facility, Newport News, VA 23606, USA

³Helmholtz-Institut für Strahlen- und Kernphysik der Universität Bonn, Nußallee 14-16, 53115 Bonn, Germany

⁴Bethe Center for Theoretical Physics, Universität Bonn, 53115 Bonn, Germany

Abstract. Recent progress in baryon spectroscopy is reviewed. In a common effort, various groups have analyzed a set of new high-precision polarization observables from ELSA. The Jülich-Bonn group has finalized the analysis of pion-induced meson-baryon production, the photoproduction of pions and eta mesons, and (almost) the $K\Lambda$ final state. As data become preciser, statistical aspects in the analysis of excited baryons become increasingly relevant and several advances in this direction are proposed.

1 Introduction

Increasingly accurate data is produced from photoproduction experiments, allowing for much improved amplitude analyses. Double polarization observables are being released that allow to reduce ambiguities and uncertainties of multipole solutions. In addition, more and more final states like ηN and KY are measured that be simultaneously analyzed using multi-channel partial-wave analysis techniques. As a result, resonance properties are determined to greater precision allowing for improved comparison with theory.

Yet, the multipoles extracted by different groups differ from each other because different parameterizations are used, the analyzed data bases are different, and the quality of the fits (χ^2 or likelihood) is different. On top of this, the different groups treat systematic uncertainties differently. Given the spectacular experimental progress in recent years, it becomes, therefore, desirable to address these problems.

To check whether the data themselves can help to reduce discrepancies in different multipole solutions, the SAID, MAID, Bonn-Gatchina and Jülich-Bonn groups teamed up to compare solutions before and after the inclusion of new high-precision π^0 photoproduction data produced at ELSA [1–4]. The quality of the fits to the new data is similar as shown in Ref. [5].

Comparing the multipoles, the visual inspection already indicates that solutions came closer to each other. We have also quantified this by calculating the pairwise and overall variances between the SAID, Bonn-Gatchina, and Jülich-Bonn solutions before and after the inclusion of the new data. That variance, at a given energy, is defined as the sum over the squared differences in all multipoles up to an angular momentum of the final state of $L = 4$. In Fig. 1

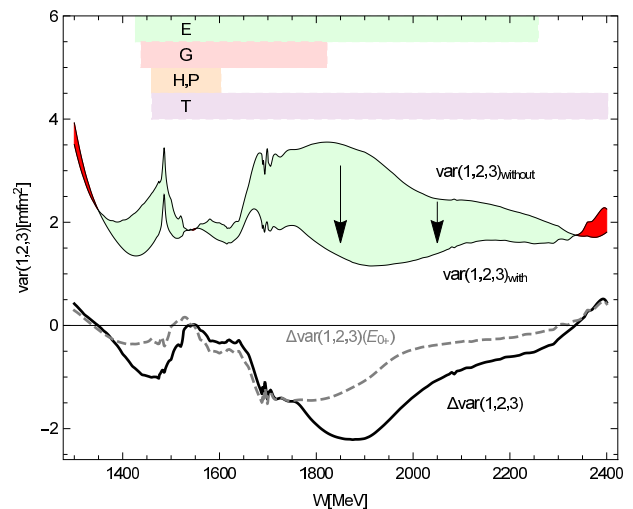


Figure 1. The variance of all three PWAs summed over all $\gamma p \rightarrow \pi^0 p$ multipoles up to $L = 4$ [5]. The range covered by the new double polarization observables [1–4] are indicated by shaded areas. Over the largest part of the energy range the new data have enforced an improvement of the overall consistency. The improvement is displayed as light green area and, separately as difference of the variance. The contribution to the improvement from the E_{0+} wave is shown as the dashed curve. Ranges with an overall deterioration are marked in red.

the the overall variance is shown as a function of total energy. Indeed, in the energy region covered by the new high precision data, discrepancies are substantially reduced as indicated with the arrows in the upper part of the figure. The solid line in the lower part shows the change, while the dashed line indicates the change from the E_{0+} multipole alone. At lower energies, the solutions come closer to each other even outside the window covered by the new

*e-mail: doring@gwu.edu

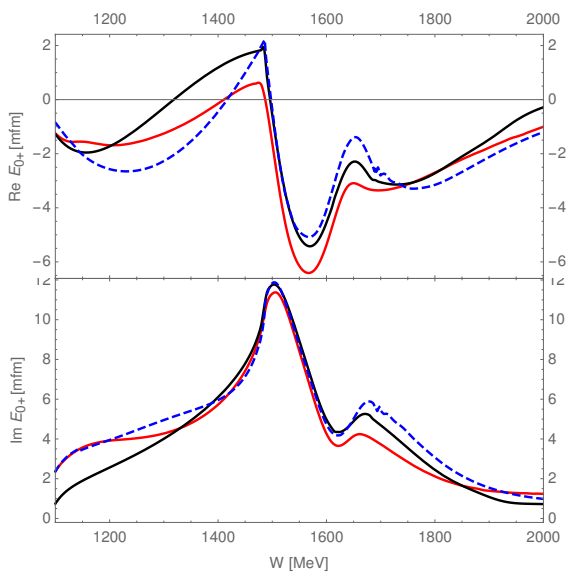


Figure 2. The E_{0+} multipole after inclusion of new $\pi^0 p$ observables [1–4]. Black solid line: BnGa, blue dashed lines: JüBo, red solid lines: SAID.

data, while at very low and high energies solutions show slightly larger discrepancies (red areas).

This is a clear indication that indeed high precision data help to determine multipoles more precisely and remove discrepancies between the solutions of different groups. A large part of the reduction in variance originates from the E_{0+} multipole. In Fig. 2 this multipole, after inclusion of the new data in the fits, is shown. It is apparent that despite the qualitative agreement, the details of the multipoles are still different. Most visible is the difference in the description of the cusp in $\text{Re } E_{0+}$ at the ηN threshold. In conclusion, while new high-precision data significantly reduce discrepancies among different partial-wave analysis groups, the details show that it is too early to state perfect matching.

The analysis of photoproduction data could also benefit from improved data on pion-induced reactions, as recently achieved for elastic pion-nucleon scattering [6]. In Ref. [7] the data on the reactions $\pi N \rightarrow \eta N, KY$ were discussed and analyzed. For example, the measured observables $d\sigma/d\Omega$, P , and β for the reaction $\pi N \rightarrow K\Lambda$ provide, in principle, a complete experiment up to a discrete ambiguity. However, the data are in many cases conflicting, in general not very precise, or even known to be problematic as in $\pi N \rightarrow \eta N$ at higher energies. Re-measurements of these reactions would be desirable and provide complementary information on the baryon spectrum. Physics opportunities with hadron beams have been discussed in Ref. [8].

2 Analysis of η and $K\Lambda$ photoproduction

The Jülich-Bonn group (JüBo) has performed comprehensive analyses of pion photoproduction [9], η photoproduc-

tion [10] and $K\Lambda$ photoproduction [11]. In several occasions, the group has analyzed new experimental data that were then published together with the analyses [12, 13]. The amplitude used for these analysis is based on a field-theoretical framework using chiral interactions. For a description of the approach, see, e.g., Ref. [7].

As an example for the current progress, analyzed observables in kaon photoproduction at selected energies are shown in Fig. 3. The two curves correspond to solutions with a new $P13(1900)$ resonance (red solid lines) and without (blue dash-dotted lines). A final assessment whether the improvement of the fit through this state is significant will follow soon. The Bonn-Gatchina, Giessen, and other analyses include this state [14, 15].

Another interesting observable is shown in Fig. 4. The E observable in the reaction $\gamma p \rightarrow \eta p$ has been recently measured by the CLAS collaboration [13] for the first time ever. The different lines correspond to two fits to differently binned data. The open circles show the fit result if the finite bin width is corrected for. There is a clear structure slightly below $W = 1.7$ GeV. However, in the analysis it was found that the structure can be explained as a conventional effect from the interference of a few multipoles, and no new narrow structure is needed for the description of the data [13].

3 Developments for future analyses

3.1 Statistical meaning of πN partial waves

A notorious problem in multi-channel analyses is to statistically quantify the significance of, e.g., a new resonance. In order to build on the progress made in the earlier πN elastic analyses, multi-channel analyses have usually fitted πN amplitudes, derived from previous studies [16], together with measured data on other reactions. The fitted amplitude pseudo-data have either been taken from single-energy analyses (SE) or energy-dependent (ED) fits covering the resonance region. The SE analysis amplitudes, derived from fits to narrow energy bins of data, have associated errors which have been used in the multi-channel fits, or enlarged when these fits have become problematic. The smoother ED amplitudes have also been taken at discrete energies, typically with subjective errors not derived from the fit to data.

There are several problems associated with fits to amplitude pseudo-data, which were recently addressed in Ref. [17]. The most obvious of these is the fact that the goodness of fit to these sets of amplitudes cannot be translated into a quality of fit to the underlying dataset. In addition, uncertainties on the SE amplitudes [16] do not account for correlated errors, which can be substantial in some cases.

In baryon spectroscopy, based on multi-reaction analysis, this has unwanted side effects. First, a statistical analysis of fit results is difficult if one of the input channels is not given by data providing a meaningful χ^2 . Second, as a consequence, the significance of resonance signals, detected in such multi-reaction fits, is difficult to quantify.

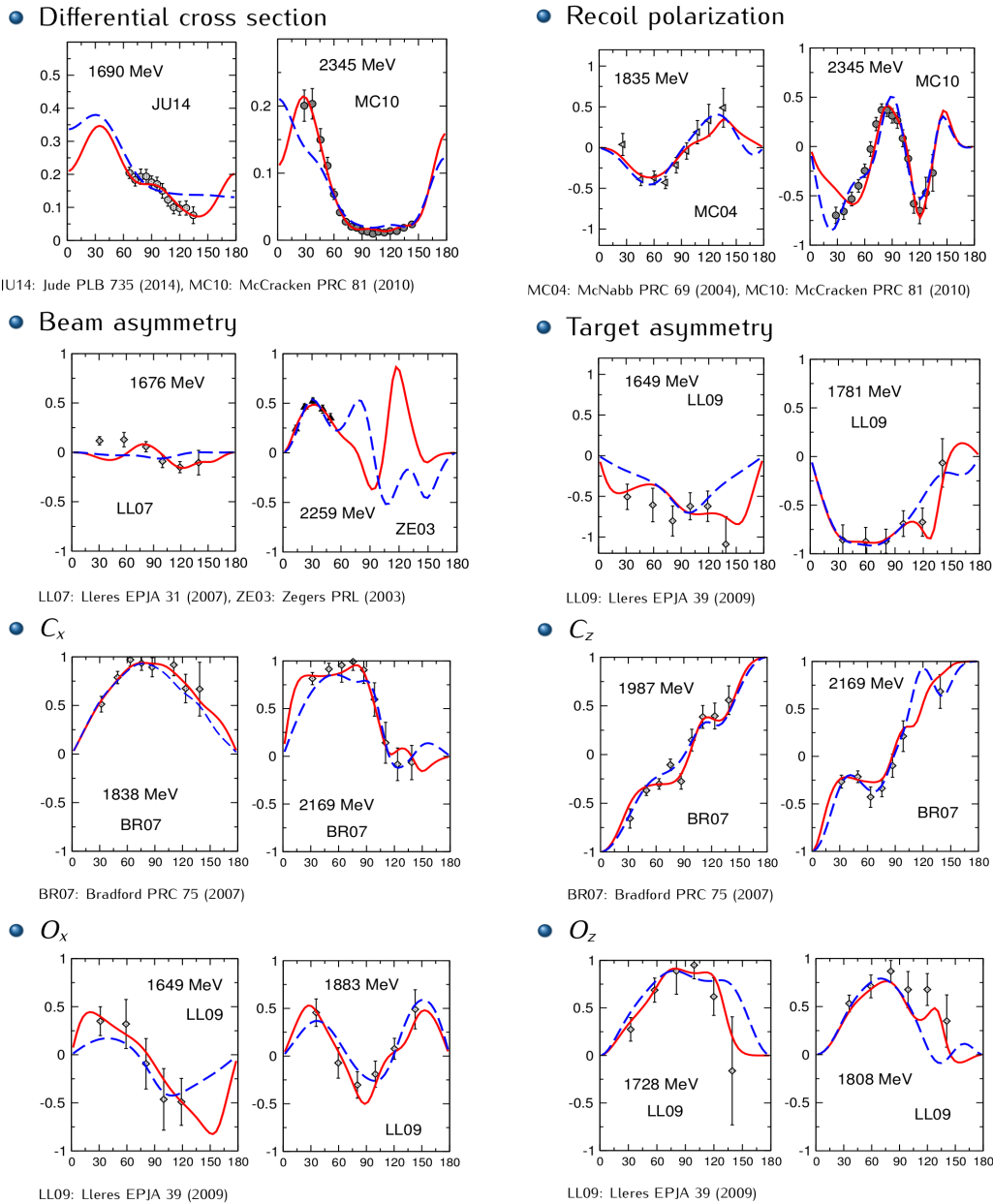


Figure 3. Selected results for the preliminary analysis of kaon photoproduction. The red lines show the best fit with a new $P13(1900)$ resonance, the blue dashed lines without.

In Ref. [17], the covariance matrices of the SE solutions have been calculated, plus additional quantities needed to perform correlated χ^2 fits, overcoming the mentioned problem. In that way, other groups can continue using the partial wave solutions of the SAID group for their multi-channel fits, and, at the same time, the χ^2 returned in such fits is very close to the one as if $\pi N \rightarrow \pi N$ data were fitted directly.

3.2 Model selection techniques

As discussed, discrepancies among different partial-wave analyses are reduced once high-precision polarization data are included in the analyses. Second, to better judge the uncertainties in a given analysis, the inclusion of elastic

pion-nucleon scattering can be improved as discussed in the previous section. Yet, to obtain a reliable spectrum of excited baryons and their properties, it is necessary to make a selection of how many resonance states should be included in the model amplitude. In particular, for broad resonances this is not clear at all because, maybe, a very similar data description could be obtained by a background term instead of a resonance term. In the SAID analysis [16] the selection process is data driven, because resonances are generated only if required by data and no manual intervention is needed. In any case, it would be desirable to aim at solutions that, with a minimum of resonances, describe the data well. Blindfolding the model selection with the bias of minimal resonance content is therefore a way to exclude solutions that are over-populated

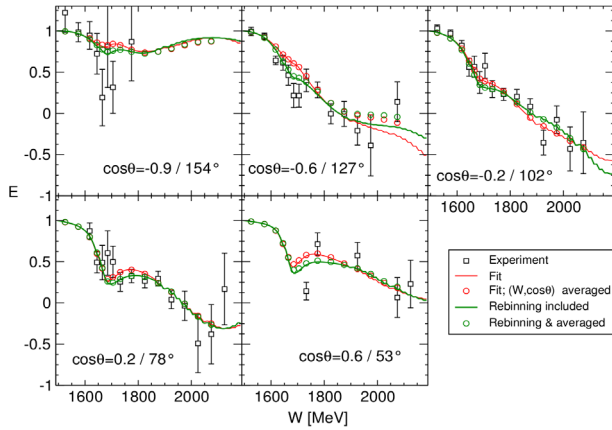


Figure 4. The E observable in $\gamma p \rightarrow \eta p$ as measured by the CLAS collaboration [13] for the first time. The different lines correspond to two fits to differently binned data. The open circles show the fit result if the finite bin width is corrected for.

with resonances. Model selection can be performed by penalizing the occurrence of resonances through additional terms in the χ^2 . A very successful method is provided by the so-called LASSO (least absolute shrinkage and selection operator) [18, 19]. However, the size of the penalty is a-priori not determined - obviously, too large of a penalty will remove all resonances from the amplitude while too small of a penalty will lead to an overpopulated spectrum. Therefore, the LASSO penalty parameter needs to be determined by an independent method, in the context of data analysis from cross validation or information theory [19].

Based on an existing model of the $\bar{K}N \rightarrow K\Xi$ reaction [20], we are performing a test of principle using the LASSO. Indeed, by starting with a largely over-populated resonance amplitude, the LASSO finds exactly those resonances significant that were singled out in Ref. [20] by hand in extensive tests of resonance combinations. A publication is in preparation.

Yet, a caveat tied to the discussed techniques remains: Many of the data in pion- and photon-induced reactions are contradictory or systematic errors are underestimated. To achieve progress in baryon spectroscopy in the discussed directions, it is there necessary to re-assess the data base.

3.3 Complex systems in the finite volume

It is, in any case, interesting to note that the discussed model selection techniques can also be used in the analysis of data from lattice QCD calculations. In Ref. [21] the problem of extrapolating lattice QCD results, obtained in a small volume, to the infinite volume is discussed. In particular, a quantity known from nuclear physics, the optical potential, is proposed to serve for this step. Fig. 5 shows an example. To demonstrate the principle, in a numerical simulation we have evaluated the optical potential in the finite volume using a known amplitude for coupled-channel $\pi\eta$, $K\bar{K}$ scattering. The real-valued potential is shown in Fig. 6 with the gray dashed line. It is char-

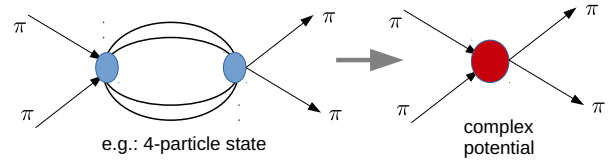


Figure 5. Optical potential. Formally, multi-particle and multi-channel scattering problems can be rewritten in terms of one channel and an optical potential that encodes the complexity of the scattering problem. In the figure, a four-pion state is absorbed into the (complex) optical potential.

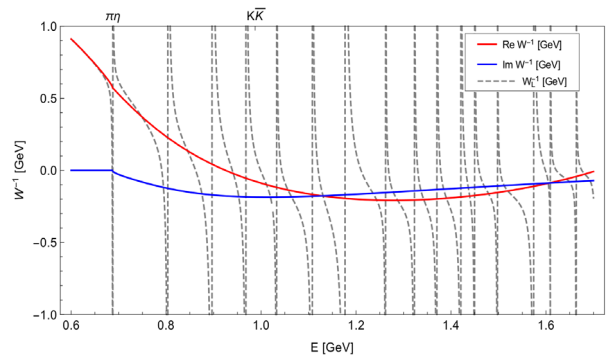


Figure 6. The real-valued optical potential for $\pi\eta$, $K\bar{K}$ scattering in the finite volume (gray dashed line). In the infinite volume, the optical potential (red line) develops also an imaginary part (blue line).

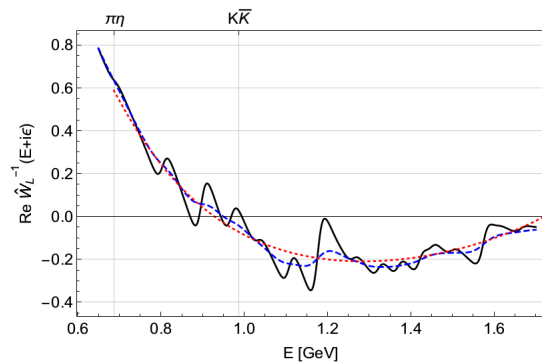


Figure 7. Real part of the optical potential in the finite volume, at complex energies $E \rightarrow E + i\epsilon$ for $\epsilon = 20$ MeV (black solid line) and $\epsilon = 50$ MeV (blue dashed line). The infinite-volume optical potential is shown with the red dotted line.

acterized by finite-volume artefacts in form of multiple poles. In contrast, the infinite-volume optical potential, using the same underlying physical process, is smooth up to threshold openings and has an imaginary part as the figure shows. This demonstrates that the limit $L \rightarrow \infty$ (where L is the side length of the finite cubic volume) is not straightforward to take. Instead, the limit is well-defined for small imaginary parts $E \rightarrow E + i\epsilon$. For such finite ϵ , Fig. 7 shows the real part of the optical potential (the imaginary part shows a similar behavior). At complex energies, the

poles on the real axis appear as oscillations. Considering the infinite-volume optical potential at the same time (red dotted line in the figure) it becomes clear that the $L \rightarrow \infty$ extrapolation can be obtained by smoothing the oscillations originating from the finite volume.

The problem is now reduced to smoothing a highly oscillatory curve with a low-order polynomial or a different suitable parameterization. A way to achieve this is, again, provided by the LASSO method. In this context, the second derivative of the curve is penalized such that smooth functions are preferred. In combination with cross validation, it was shown in Ref. [21] that it is indeed possible to reconstruct the infinite-volume optical potential from lattice data obtained in the finite volume.

Future applications of this method become increasingly relevant, because finite-volume artefacts get large at smaller quark masses close to the physical point. Second, lattice simulations are now at the verge of moving beyond the simplest hadronic systems addressing multi-channel and multi-particle states. The optical potential can absorb the corresponding degrees of freedom and represents, thus, a promising technique in the analysis of future lattice QCD simulations.

4 Summary

Progress in the analysis of pion and photon-induced reactions has been made in the last years. Using a coupled-channel approach based on field theory, the Jülich-Bonn group extracted amplitudes and resonance properties from the world data of pion and eta photoproduction. The fit to $K\Lambda$ data is finished.

To get closer to definite answers regarding the spectrum of excited baryons, new methods were proposed addressing mainly the statistical aspect of analysis, that will become increasingly relevant given recent and future high-precision data. One aspect concerns the need to perform entirely data-driven analyses, for which the necessary information within the SAID approach has been calculated and made available. Model selection techniques can be used to derive amplitudes with a minimal resonance content and minimize the danger of false-positive resonance signals. These techniques are applicable not only in baryon spectroscopy but also in the analysis of lattice QCD data, in particular through the use of the optical potential in the infinite-volume extrapolation of complex hadronic systems that have become into the reach of ab-initio QCD calculations.

Acknowledgements: The authors gratefully acknowledge the computing time granted on the supercomputer JURECA at Jülich Supercomputing Centre (JSC). This work is also partially supported by the DFG (Deutsche Forschungsgemeinschaft) and NSFC through the Sino-German CRC 110 (“Symmetries and the Emergence of

Structure in QCD”). M.M. is supported by a DFG research fellowship (MA 7156/1-1). M.D. is supported by the National Science Foundation (PIF grant No. PHY 1415459 and CAREER grant No. 1452055) and by the U.S. Department of Energy, Office of Science, Office of Nuclear Physics under contract DE-AC05-06OR23177.

References

- [1] J. Hartmann *et al.* [CBELSA/TAPS Collaboration], *Phys. Lett. B* **748** (2015) 212.
- [2] A. Thiel *et al.*, arXiv:1604.02922 [nucl-ex].
- [3] M. Gottschall *et al.* [CBELSA/TAPS Collaboration], *Phys. Rev. Lett.* **112** (2014), 012003.
- [4] A. Thiel *et al.*, *Phys. Rev. Lett.* **109** (2012) 102001.
- [5] R. Beck *et al.*, arXiv:1604.05704 [nucl-th], accepted for publication in *Eur. Phys. J. A*.
- [6] A. Gridnev *et al.* [EPECUR Collaboration], *Phys. Rev. C* **93** (2016), 062201.
- [7] D. Rönchen *et al.*, *Eur. Phys. J. A* **49** (2013) 44.
- [8] W. J. Briscoe, M. Döring, H. Haberzettl, D. M. Manley, M. Naruki, I. I. Strakovsky and E. S. Swanson, *Eur. Phys. J. A* **51** (2015), 129.
- [9] D. Rönchen *et al.*, *Eur. Phys. J. A* **50** (2014), 101 Erratum: [*Eur. Phys. J. A* **51** (2015), 63].
- [10] D. Rönchen, M. Döring, H. Haberzettl, J. Haidenbauer, U.-G. Meißner and K. Nakayama, *Eur. Phys. J. A* **51** (2015), 70.
- [11] D. Rönchen *et al.*, publication in preparation.
- [12] S. Strauch *et al.* [CLAS Collaboration], *Phys. Lett. B* **750** (2015), 53.
- [13] I. Senderovich *et al.* [CLAS Collaboration], *Phys. Lett. B* **755** (2016), 64.
- [14] E. Gutz *et al.* [CBELSA/TAPS Collaboration], *Eur. Phys. J. A* **50** (2014), 74.
- [15] V. Shklyar, H. Lenske and U. Mosel, *Phys. Rev. C* **87** (2013), 015201.
- [16] R. L. Workman, R. A. Arndt, W. J. Briscoe, M. W. Paris and I. I. Strakovsky, *Phys. Rev. C* **86** (2012), 035202.
- [17] M. Döring, J. Revier, D. Rönchen and R. L. Workman, *Phys. Rev. C* **93** (2016), 065205.
- [18] B. Guegan, J. Hardin, J. Stevens and M. Williams, *JINST* **10** (2015), P09002.
- [19] *The Elements of Statistical Learning: Data Mining, Inference, and Prediction*, T. Hasti, R. Tibshirani, J. Friedman, Springer 2009, second edition.
- [20] B. C. Jackson, Y. Oh, H. Haberzettl and K. Nakayama, *Phys. Rev. C* **91** (2015), 065208.
- [21] D. Agadjanov, M. Döring, M. Mai, U.-G. Meißner and A. Rusetsky, *JHEP* **1606** (2016) 043.